Supplementary Materials for: Comparative Evaluation of ERA5-Land and ISIMIP3 Runoff Forcing for Global River Streamflow Simulation

Julien E. S. Boulange[1], Fang Zhao[2], Simon N. Gosling[3], Yadu Pokhrel[4], Dai Yamazaki[5], Xudong Zhou[6]

[1] United graduate school of agricultural science, Tokyo University of Agriculture and Technology, Fuchu, Tokyo, Japan

[2] Key Laboratory of Geographic Information Science of the Ministry of Education, School of Geographic Sciences, East China Normal University, Shanghai 200241, China.

[3] School of Geography, University of Nottingham, UK

[4] Department of Civil and Environmental Engineering, Michigan State University, USA

[5] Global Hydrological Prediction Center, Institute of Industrial Science, The University of Tokyo, Tokyo, Japan

[6] Institute of Hydraulic and Ocean Engineering, Ningbo University, Ningbo, China

Correspondence to: Julien Boulange (boulange@go.tuat.ac.jp) and Fang Zhao (fzhao87@foxmail.com)

List of Supplementary Sections

List of Supplementary Tables

List of Supplementary Figures

Fig. S3: Spatial distribution of the best-performing ISIMIP3a hydrological model across IPCC SREX regions. The best model is defined for each region based on its performance in reproducing observed daily streamflow using the *KGE* metric.

Fig. S4: Comparison of Kling–Gupta Efficiency (*KGE*) scores at the station level between simulations forced with original ERA5-Land data and ERA5-Land data upscaled to 0.5° resolution. Each point represents an individual gauging station. The dashed line indicates the 1:1 relationship.

Fig. S5: Comparison of Kling–Gupta Efficiency (*KGE*) components between the ERA5-Land simulation and the upscaled ERA5-Land forcing across all stations. Each panel shows a different component (correlation, variability ratio, and bias), with points representing individual stations. The dashed line indicates the 1:1 relationship. Reported Pearson correlation coefficients (*R*) and associated *p*-values are shown for each component. For clarity, extreme bias values were excluded from the visualization.

Fig. S6: Spatial distribution of the median bias component (β) of the Kling–Gupta Efficiency (*KGE*) for ISIMIP3a hydrological models across IPCC SREX regions. A value of $\beta = 1$ indicates unbiased simulations, while values below (above) 1 indicate systematic underestimation (overestimation) of streamflow.

Fig. S7: Spatial distribution of the median variability component (α) of the Kling–Gupta Efficiency (*KGE*) for ISIMIP3a hydrological models across IPCC SREX regions. A value of $\alpha = 1$ indicates correct representation of streamflow variability, while values below (above) 1 indicate systematic underestimation (overestimation) of variability.

Fig. S8: Spatial distribution of the median correlation component (r) of the Kling–Gupta Efficiency (*KGE*) for ISIMIP3a hydrological models across IPCC SREX regions. The correlation coefficient (r) reflects the temporal agreement between simulated and observed streamflow, with higher values indicating better reproduction of flow dynamics.

Fig. S9: Comparison of the trends in streamflow between the ERA5-Land simulation and the upscaled ERA5-Land forcing across all stations. Each panel shows a different streamflow regime (low, mean, and high), with points representing individual stations. The dashed line indicates the 1:1 relationship. Reported Pearson correlation coefficients (*R*) and associated *p*-values are shown for each component.

Supplementary References

Supplementary Sections

Section S1: Previous assessments of ERA5-Land

The evaluation of reanalysis datasets, including ERA5-Land, has largely focused on variables such as precipitation, snow cover, temperature, and wind speed. ERA5-Land precipitation has been shown to reasonably capture the spatial patterns and seasonal dynamics across large regions, including China (Xie et al., 2022), the contiguous United States (Smith et al., 2025), and European countries (Gomis-Cebolla et al., 2023). Nonetheless, biases have been reported, particularly in the simulation of light (Li et al., 2025) and extreme (Clelland et al., 2024) precipitation events, although performance in capturing heavy rainfall has been found adequate is some regions (Tan et al., 2023).

With respect to runoff, ERA5-Land has demonstrated adequate performance globally, especially in regions such as Central Europe, India, the southern United States, and the Amazon (Chaudhari and Pokhrel, 2022; Dutta and Markonis, 2024). However, limitations remain in arid and semi-arid regions, where accuracy is notably reduced (Dutta and Markonis, 2024). In addition, in the Tibetan permafrost region, ERA5-Land runoff was able to capture interannual variability but systematically underestimated the runoff recession rate (Liu et al., 2024), possibly due to deficiencies in simulated precipitation amount and frequency, also highlighted for some high mountains in Asia (Sun et al., 2021; Wu et al., 2023) and in the Mekong region (Dang and Pokhrel, 2024). Despite these regional discrepancies, ERA5-Land remains the reference benchmark for runoff data in global hydrological applications, reflecting its overall reliability and broad applicability (Hamitouche et al., 2025).

Section S2: Sensitivity of trend correlations to influential regions

To assess whether cross-regional correlations between simulated and observed streamflow trends were disproportionately influenced by a small number of regions with strong signals, we performed a leave-one-out analysis in which correlations were recalculated after sequentially excluding each SREX region (Table S2).

Supplementary Tables

Table S1: Overview of the global hydrological models included in the ISIMIP3a ensemble, including model names, key references, and schematic representations of soil water balance processes. Equations and processes' names adapted from Telteu et al., (2021). Additional model specific information is available here: https://www.isimip.org/impactmodels/.

GHM model	Soil storage	Key reference(s)
CLASSIC	$\frac{\delta S_{so}}{\delta t} = \begin{cases} M + P_{th} + R_{in,i} - E_{so,i} - R_{gwr,i} - R_{su} & i = 0 \\ R_{gwr,i-1} - R_{gwr,i} - R_{if} & i > 0 \end{cases}$	Melton et al., (2020)
CWatM	$\frac{\delta S_{so}}{\delta t} = R_{cr} + R_{in} - R_{gwr} - R_{if} - E_{so} - T$	Burek et al., (2020)
H08	$\frac{\delta S_{so,i}}{\delta t} = M + P_{th} - E_{so} - R_{in}$	Hanasaki et al., (2018); Yoshida et al., (2022)
HydroPy	$\frac{\delta S_{so}}{\delta t} = R_{in} - R_{pe} - E_{so} - T$	Stake and Hagemann (2021)
JULES-W2	$\frac{\delta S_{so}}{\delta t} = M + P_{th} - E_{so} - R_{if} - R_{in}$	Best et al., (2011); Tsilimigkras et al., (2025)
MIROC-INTEG-LAND	$\frac{\delta S_{so}}{\delta t} = \sum_{n=1,13} \left[\left(S_{so,Fi} + S_{SO,uFi} \right) \times d_{so} \right]$	Yokohata et al., (2020)
ORCHIDEE-MICT	$\frac{\delta S_{so}}{\delta t} = R_{in} - R_{in,r} - R_{su} - E_{so}$	Guimberteau et al., (2018)
WaterGAP2-2e	$\frac{\delta S_{so}}{\delta t} = R_{in} - R_{tot} - E_{so}$	Müller Schmied et al., (2021, 2024)
WEB DHM-SG	$\frac{\delta S_{so}}{\delta t} = \begin{cases} R_{in,i} - E_{so,i} - R_{gwr,i} & i = 0 \\ R_{gwr,i-1} - R_{gwr,i} - T_i & i > 0 \end{cases}$	Qi et al., (2022)

where: S_o (L^3L^{-2}) is the soil water storage compartment; $S_{o,i}$ (L^3L^{-2}) is the soil water storage in layer i; M ($L^3L^{-2}T^{-1}$) is the amount of snowmelt; P_{th} ($L^3L^{-2}T^{-1}$) is throughfall or total precipitation that falls to the ground through canopy spaces; E_{so} ($L^3L^{-2}T^{-1}$) is soil evaporation; T ($L^3L^{-2}T^{-1}$) is transpiration; R_{cr} ($L^3L^{-2}T^{-1}$) is capillary rise; R_{in} ($L^3L^{-2}T^{-1}$) is water infiltration; $R_{in,r}$ ($L^3L^{-2}T^{-1}$) is water re-infiltration; R_{if} ($L^3L^{-2}T^{-1}$) is interflow or subsurface flow; R_{su} ($L^3L^{-2}T^{-1}$) is surface runoff or overland flow; R_{gwr} ($L^3L^{-2}T^{-1}$) is groundwater recharge; R_{tot} ($L^3L^{-2}T^{-1}$) is total runoff from land (includes surface runoff, subsurface runoff, and groundwater recharge); $S_{so,Fi}$ (L^3L^{-2}) is the frozen soil water moisture at layer index i; $S_{so,uFi}$ (L^3L^{-2}) is the unfrozen soil moisture at layer index i; d_{so} (L) is the total soil depth.

Table S2: Range of leave-one-out cross-regional Pearson correlation coefficients between observed and simulated regional streamflow trends after sequential exclusion of each SREX region.

Dataset	Low	Mean	High
ERA5-Land	0.794–0.895	0.779–0.899	0.871–0.914
ISIMIP3a	0.731–0.903	0.733–0.842	0.746–0.861
Best performing models	0.582–0.763	0.647–0.810	0.629–0.809

Supplementary Figures

Fig. S1: Spatial distribution of Global Runoff Data Centre (GRDC) streamflow stations (black dots) and number of stations aggregated within each IPCC SREX region. Shading indicates the total number of stations per region, shown only for regions with at least 80 stations. Region boundaries follow the IPCC SREX definition.

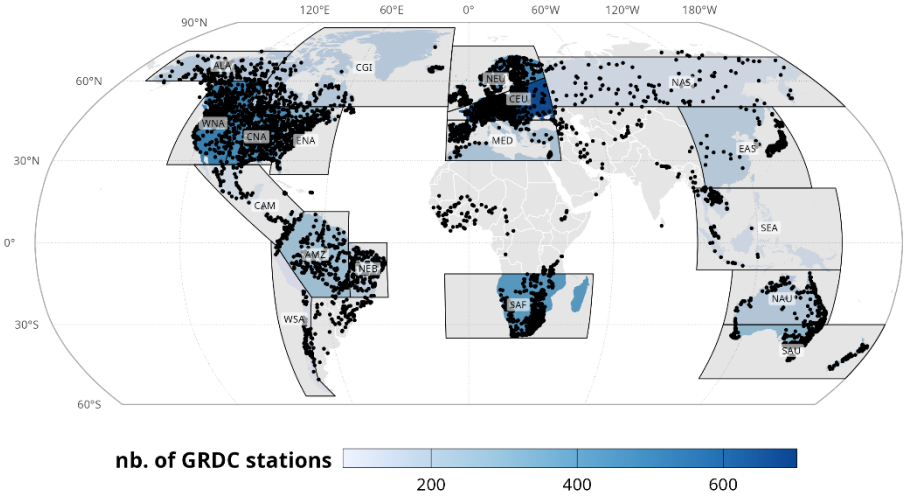

Fig. S2: Spatial distribution of median Kling–Gupta Efficiency (*KGE*) for individual ISIMIP3a hydrological models across IPCC SREX regions.

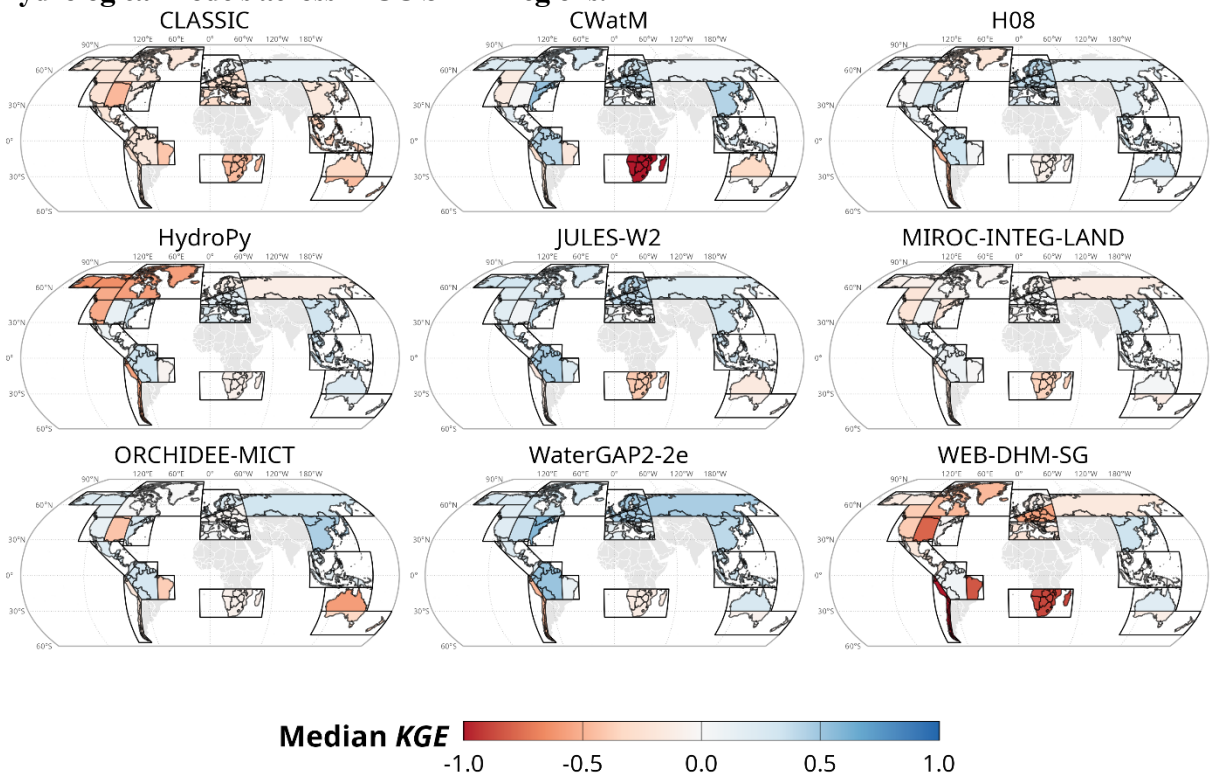

Fig. S3: Spatial distribution of the best-performing ISIMIP3a hydrological model across IPCC SREX regions. The best model is defined for each region based on its performance in reproducing observed daily streamflow using the *KGE* metric.

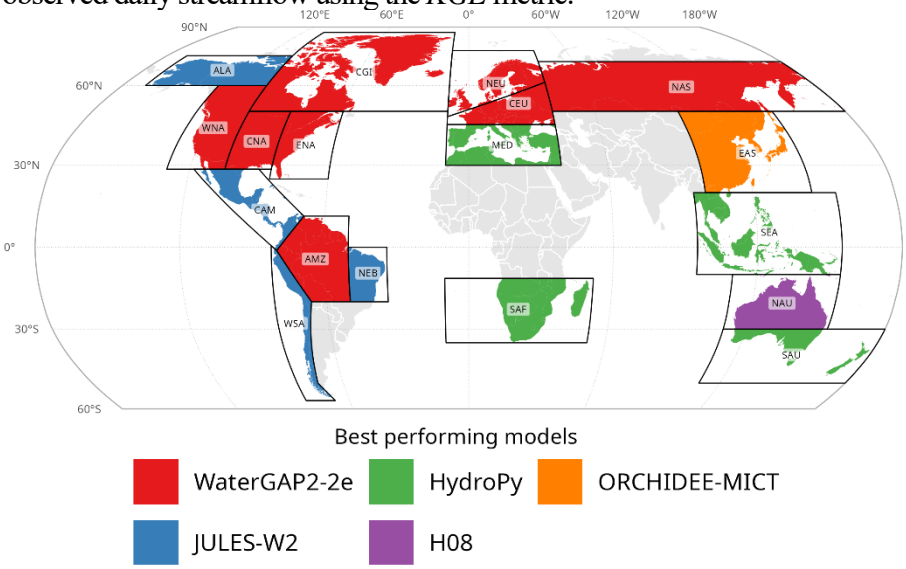

Fig. S4: Comparison of Kling–Gupta Efficiency (*KGE*) scores at the station level between simulations forced with original ERA5-Land data and ERA5-Land data upscaled to 0.5° resolution. Each point represents an individual gauging station. The dashed line indicates the 1:1 relationship.

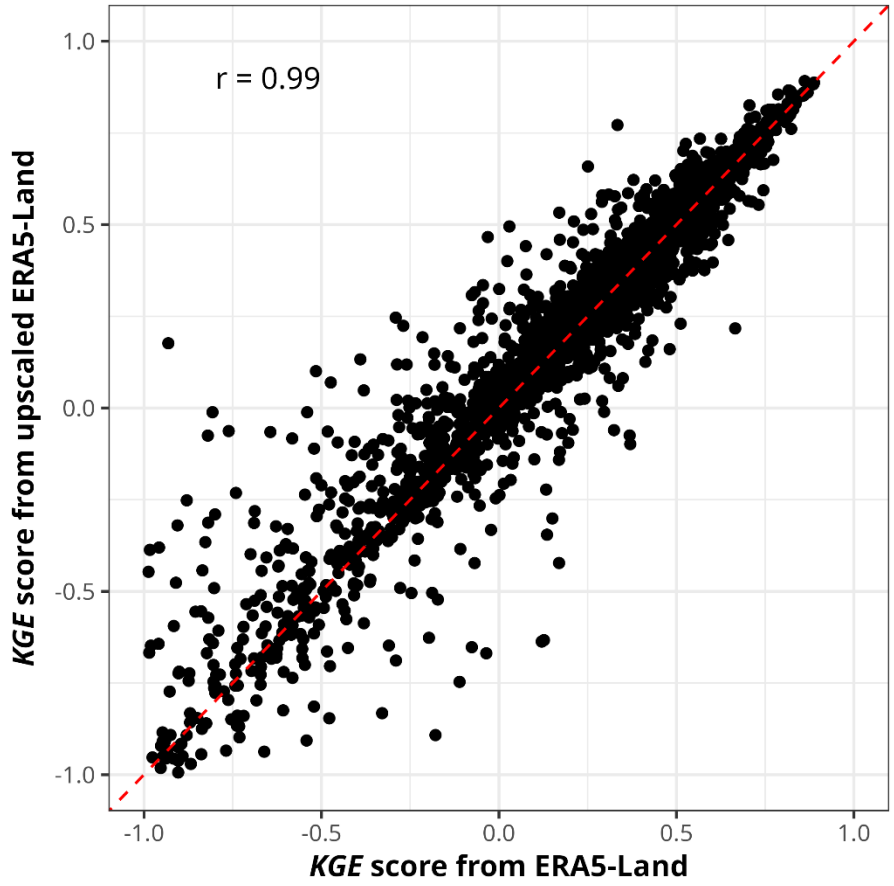

Fig. S5: Comparison of Kling–Gupta Efficiency (*KGE*) components between the ERA5-Land simulation and the upscaled ERA5-Land forcing across all stations. Each panel shows a different component (correlation, variability ratio, and bias), with points representing individual stations. The dashed line indicates the 1:1 relationship. Reported Pearson correlation coefficients (*R*) and associated *p*-values are shown for each component. For clarity, extreme bias values were excluded from the visualization.

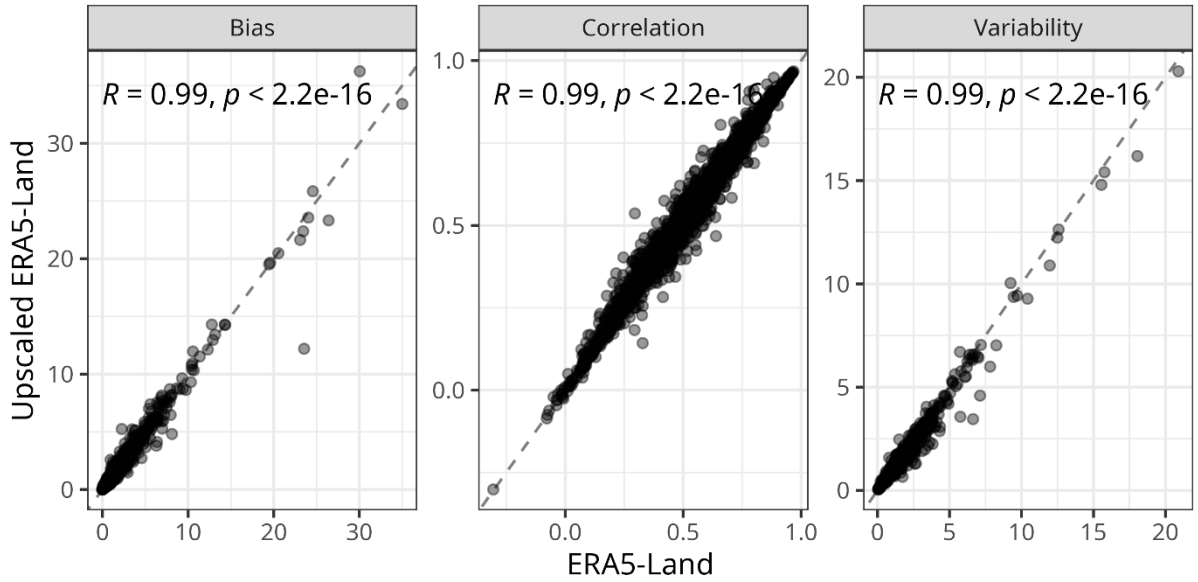

Fig. S6: Spatial distribution of the median bias component (β) of the Kling–Gupta Efficiency (*KGE*) for ISIMIP3a hydrological models across IPCC SREX regions. A value of β = 1 indicates unbiased simulations, while values below (above) 1 indicate systematic underestimation (overestimation) of streamflow.

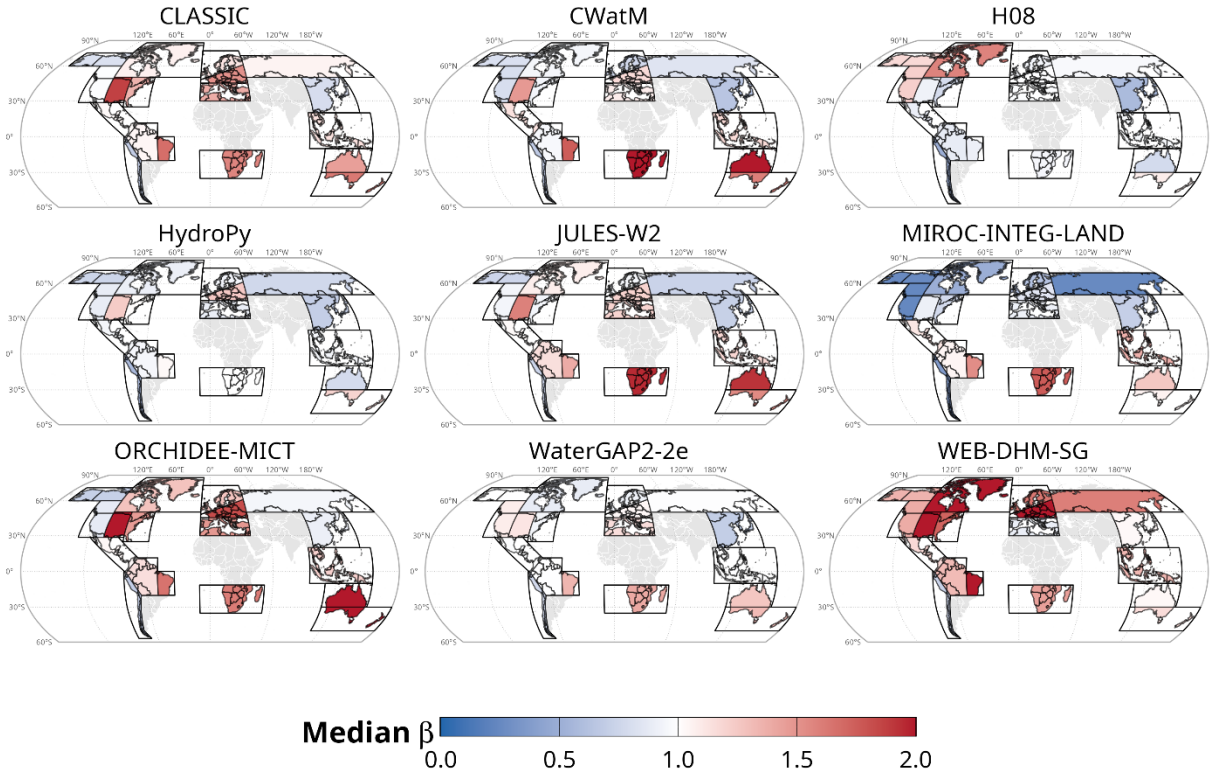

Fig. S7: Spatial distribution of the median variability component (α) of the Kling–Gupta Efficiency (*KGE*) for ISIMIP3a hydrological models across IPCC SREX regions. A value of α = 1 indicates correct representation of streamflow variability, while values below (above) 1 indicate systematic underestimation (overestimation) of variability.

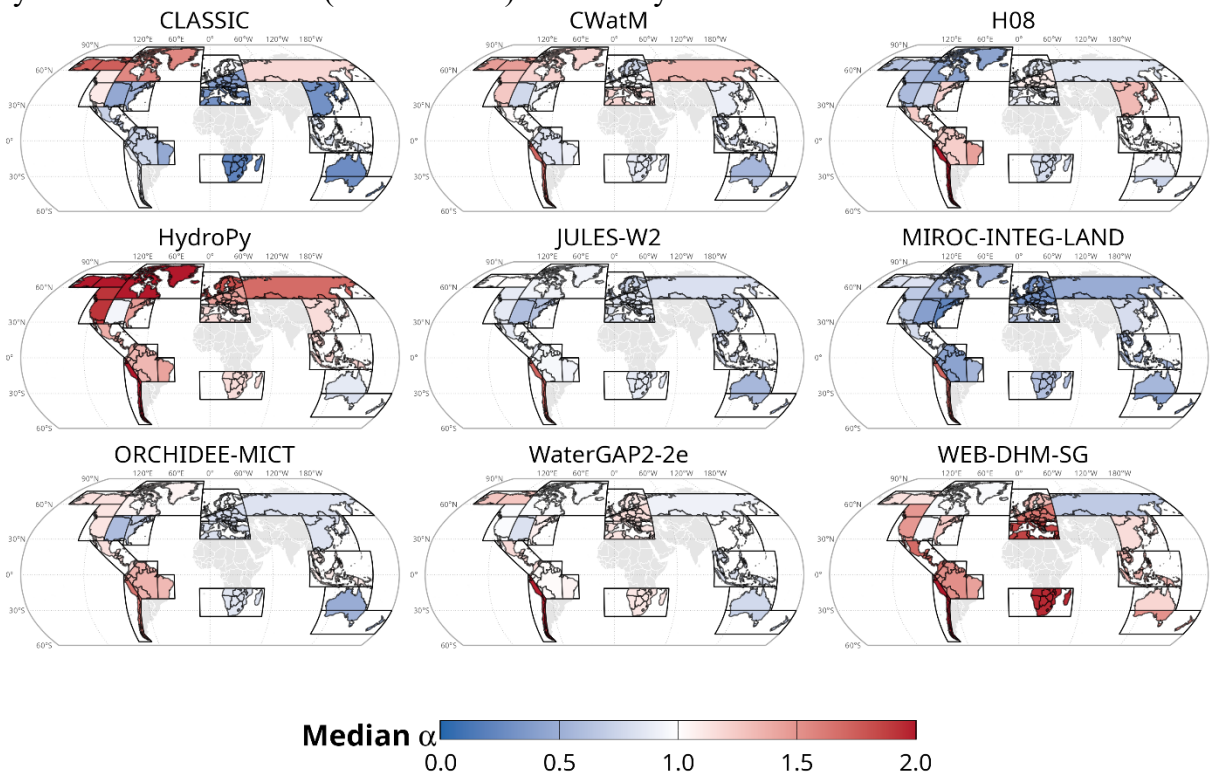

Fig. S8: Spatial distribution of the median correlation component (*r*) of the Kling–Gupta Efficiency (*KGE*) for ISIMIP3a hydrological models across IPCC SREX regions. The correlation coefficient (*r*) reflects the temporal agreement between simulated and observed streamflow, with higher values indicating better reproduction of flow dynamics.

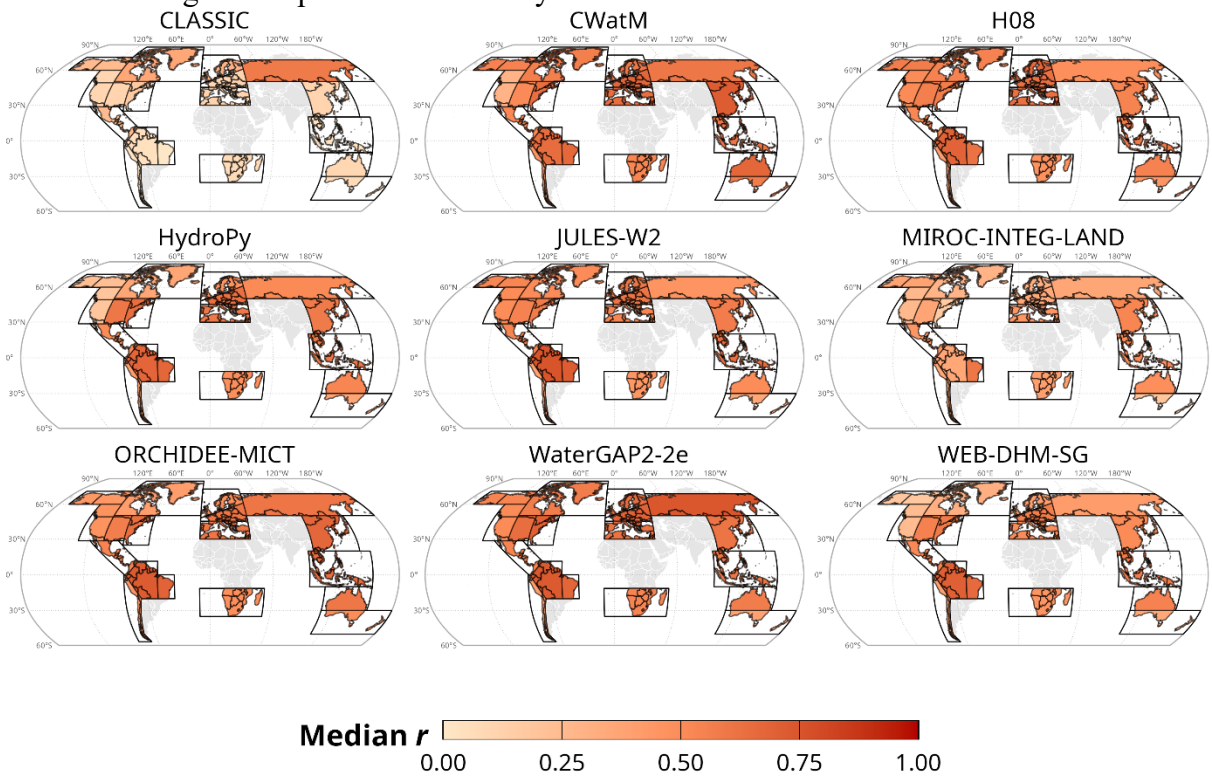

Fig. S9: Comparison of the trends in streamflow between the ERA5-Land simulation and the upscaled ERA5-Land forcing across all stations. Each panel shows a different streamflow regime (low, mean, and high), with points representing individual stations. The dashed line indicates the 1:1 relationship. Reported Pearson correlation coefficients (*R*) and associated *p*-values are shown for each component.

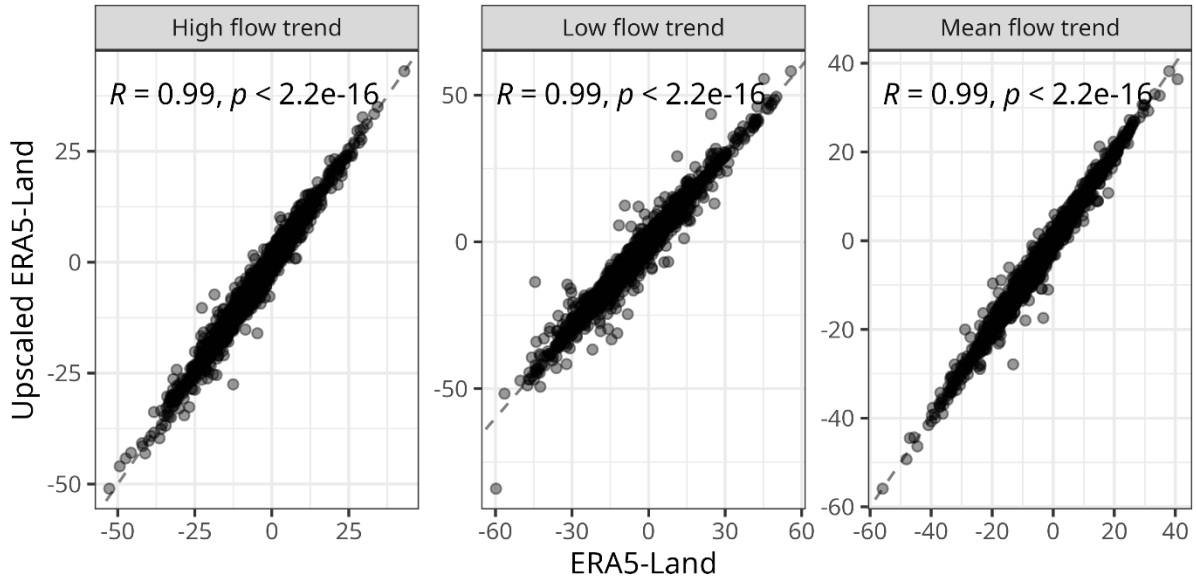

Supplementary References

Best, M. J., M. Pryor, D. B. Clark, G. G. Rooney, R. L. H. Essery, C. B. Ménard, J. M. Edwards, M. A. Hendry, A. Porson, N. Gedney, L. M. Mercado, S. Sitch, E. Blyth, O. Boucher, P. M. Cox, C. S. B. Grimmond, and R. J. Harding. 2011. "The Joint UK Land Environment Simulator (JULES), Model Description – Part 1: Energy and Water Fluxes." *Geoscientific Model Development* 4(3):677–99. doi:10.5194/gmd-4-677-2011.

Burek, P., Y. Satoh, T. Kahil, T. Tang, P. Greve, M. Smilovic, L. Guillaumot, F. Zhao, and Y. Wada. 2020. "Development of the Community Water Model (CWatM v1.04) – a High-Resolution Hydrological Model for Global and Regional Assessment of Integrated Water Resources Management." *Geoscientific Model Development* 13(7):3267–98. doi:10.5194/gmd-13-3267-2020.

Guimberteau, M., D. Zhu, F. Maignan, Y. Huang, C. Yue, S. Dantec-Nédélec, C. Ottlé, A. Jornet-Puig, A. Bastos, P. Laurent, D. Goll, S. Bowring, J. Chang, B. Guenet, M. Tifafi, S. Peng, G. Krinner, A. Ducharne, F. Wang, T. Wang, X. Wang, Y. Wang, Z. Yin, R. Lauerwald, E. Joetzjer, C. Qiu, H. Kim, and P. Ciais. 2018. "ORCHIDEE-MICT (v8.4.1), a Land Surface Model for the High Latitudes: Model Description and Validation." *Geoscientific Model Development* 11(1):121–63. doi:10.5194/gmd-11-121-2018.

Hanasaki, Naota, Sayaka Yoshikawa, Yadu Pokhrel, and S. Kanae. 2018. "A Global Hydrological Simulation to Specify the Sources of Water Used by Humans." *Hydrology and Earth System Sciences* 22(1):789–817. doi:10.5194/hess-22-789-2018.

Melton, J. R., V. K. Arora, E. Wisernig-Cojoc, C. Seiler, M. Fortier, E. Chan, and L. Teckentrup. 2020. "CLASSIC v1.0: The Open-Source Community Successor to the Canadian Land Surface Scheme (CLASS) and the Canadian Terrestrial Ecosystem Model (CTEM) – Part 1: Model Framework and Site-Level Performance." *Geoscientific Model Development* 13(6):2825–50. doi:10.5194/gmd-13-2825-2020.

Müller Schmied, H., D. Cáceres, S. Eisner, M. Flörke, C. Herbert, C. Niemann, T. A. Peiris, E. Popat, F. T. Portmann, R. Reinecke, M. Schumacher, S. Shadkam, C. E. Telteu, T. Trautmann, and P. Döll. 2021. "The Global Water Resources and Use Model WaterGAP v2.2d: Model Description and Evaluation." *Geoscientific Model Development* 14(2):1037–79. doi:10.5194/gmd-14-1037-2021.

Müller Schmied, H., T. Trautmann, S. Ackermann, D. Cáceres, M. Flörke, H. Gerdener, E. Kynast, T. A. Peiris, L. Schiebener, M. Schumacher, and P. Döll. 2024. "The Global Water Resources and Use Model WaterGAP v2.2e: Description and Evaluation of Modifications and New Features." *Geoscientific Model Development* 17(23):8817–52. doi:10.5194/gmd-17-8817-2024.

Qi, Wei, Lian Feng, Hong Yang, Junguo Liu, Yi Zheng, Haiyun Shi, Lei Wang, and Deliang Chen. 2022. "Economic Growth Dominates Rising Potential Flood Risk in the Yangtze River and Benefits of Raising Dikes from 1991 to 2015." *Environmental Research Letters* 17(3):034046. doi:10.1088/1748-9326/ac5561.

Stacke, T., and S. Hagemann. 2021. "HydroPy (v1.0): A New Global Hydrology Model Written in Python." *Geoscientific Model Development* 14(12):7795–7816. doi:10.5194/gmd-14-7795-2021.

Telteu, C. E., H. Müller Schmied, W. Thiery, G. Leng, P. Burek, X. Liu, J. E. S. Boulange, L. S. Andersen, M. Grillakis, S. N. Gosling, Y. Satoh, O. Rakovec, T. Stacke, J. Chang, N. Wanders, H. L. Shah, T. Trautmann, G. Mao, N. Hanasaki, A. Koutroulis, Y. Pokhrel, L. Samaniego, Y. Wada, V. Mishra, J. Liu, P. Döll, F. Zhao, A. Gädeke, S. S. Rabin, and F. Herz. 2021. "Understanding Each Other's Models: An Introduction and a Standard Representation of 16 Global Water Models to Support Intercomparison, Improvement, and Communication." *Geoscientific Model Development* 14(6):3843–78. doi:10.5194/gmd-14-3843-2021.

Tsilimigkras, Athanasios A., Douglas B. Clark, Andrew J. Hartley, Eleanor J. Burke, Manolis G. Grillakis, and Aristeidis G. Koutroulis. 2025. "Spatially-Varying Parametrization of the Total Runoff Integrating Pathways (TRIP) Scheme for Improved River Routing at the Global Scale." *Journal of Hydrology* 661:133477. doi:10.1016/j.jhydrol.2025.133477.

Yokohata, T., T. Kinoshita, G. Sakurai, Y. Pokhrel, A. Ito, M. Okada, Y. Satoh, E. Kato, T. Nitta, S. Fujimori, F. Felfelani, Y. Masaki, T. Iizumi, M. Nishimori, N. Hanasaki, K. Takahashi, Y. Yamagata, and S. Emori. 2020. "MIROC-INTEG-LAND Version 1: A Global Biogeochemical Land Surface Model with Human Water Management, Crop Growth, and Land-Use Change." *Geoscientific Model Development* 13(10):4713–47. doi:10.5194/gmd-13-4713-2020.

Yoshida, T., N. Hanasaki, K. Nishina, J. Boulange, M. Okada, and P. A. Troch. 2022. "Inference of Parameters for a Global Hydrological Model: Identifiability and Predictive Uncertainties of Climate-Based Parameters." *Water Resources Research* 58(2):e2021WR030660. doi:10.1029/2021WR030660.